

Neutrophils Enable Local and Non-Invasive Liposome Delivery to Inflamed Skeletal Muscle and Ischemic Heart

Junyi Che, Adrian Najer, Anna K. Blakney, Paul F. McKay, Mohamed Bellahcene, Charles W. Winter, Amalia Sintou, Jiaqing Tang, Timothy J. Keane, Michael D. Schneider, Robin J. Shattock, Susanne Sattler, and Molly M. Stevens*

Uncontrolled inflammation is a major pathological factor underlying a range of diseases including autoimmune conditions, cardiovascular disease, and cancer. Improving localized delivery of immunosuppressive drugs to inflamed tissue in a non-invasive manner offers significant promise to reduce severe side effects caused by systemic administration. Here, a neutrophil-mediated delivery system able to transport drug-loaded nanocarriers to inflamed tissue by exploiting the inherent ability of neutrophils to migrate to inflammatory tissue is reported. This hybrid system (neutrophils loaded with liposomes *ex vivo*) efficiently migrates *in vitro* following an inflammatory chemokine gradient. Furthermore, the triggered release of loaded liposomes and reuptake by target macrophages is studied. The migratory behavior of liposome-loaded neutrophils is confirmed *in vivo* by demonstrating the delivery of drug-loaded liposomes to an inflamed skeletal muscle in mice. A single low-dose injection of the hybrid system locally reduces inflammatory cytokine levels. Biodistribution of liposome-loaded neutrophils in a human-disease-relevant myocardial ischemia reperfusion injury mouse model after *i.v.* injection confirms the ability of injected neutrophils to carry loaded liposomes to inflammation sites. This strategy shows the potential of nanocarrier-loaded neutrophils as a universal platform to deliver anti-inflammatory drugs to promote tissue regeneration in inflammatory diseases.

Inflammation is implicated in the pathogenesis of many diseases including cardiovascular disease, autoimmunity, and cancer.^[1] A chronic inflammatory response may lead to irreversible tissue damage and chronic inflammatory diseases are a major cause of mortality; globally accounting for three out of five deaths.^[2] However, systemic administration of anti-inflammatory drugs is


hampered by poor bioavailability and biostability,^[3] undesirable off-target effects,^[4] and obstacles presented by biological barriers,^[5] thus motivating the development of drug delivery systems for efficient and localized delivery to affected tissue.

Nanoparticle-based drug delivery systems for the treatment of inflammation are a powerful tool to target anti-inflammatory drugs to inflamed tissues. However, efficient local delivery remains challenging. Main hurdles include sequestration of nanoparticles by phagocytic cells and biological barriers such as the endothelium hindering infiltration and accumulation in the inflamed tissue.^[6,7]

Employing immune cells for active transport of drugs and drug-loaded nanocarriers to a target site is a promising recent approach.^[8–10] Neutrophils are one of the most abundant, and also one of the first leukocytes to reach inflammatory tissue.^[11,12] Upon activation, neutrophils can form neutrophil extracellular traps (NETs) within a few hours, a defined release mechanism that enables

neutrophils to serve as a delivery system for drugs or loaded nanocarriers at early stages of inflammation.^[13] These properties of neutrophils have recently been leveraged to deliver paclitaxel-loaded liposomes to suppress postoperative glioma recurrence.^[8] Another study designed nanocarriers to attach to neutrophils and monocytes in circulation that subsequently

J. Che, Dr. A. Najer, Dr. C. W. Winter, J. Tang, Dr. T. J. Keane, Prof. M. M. Stevens
Department of Materials
Department of Bioengineering, and Institute of Biomedical Engineering
Imperial College London
London SW7 2AZ, UK
E-mail: m.stevens@imperial.ac.uk

 The ORCID identification number(s) for the author(s) of this article can be found under <https://doi.org/10.1002/adma.202003598>.

© 2020 The Authors. Published by Wiley-VCH GmbH. This is an open access article under the terms of the Creative Commons Attribution License, which permits use, distribution and reproduction in any medium, provided the original work is properly cited.

Dr. A. K. Blakney, Dr. P. F. McKay, Prof. R. J. Shattock
Department of Infectious Diseases
Imperial College London
London W2 1PG, UK

Dr. M. Bellahcene, Prof. M. D. Schneider
British Heart Foundation Centre of Research Excellence
National Heart and Lung Institute
Imperial College London
London W12 0NN, UK

A. Sintou, Dr. S. Sattler
National Heart and Lung Institute
Imperial College London
London W12 0NN, UK

DOI: 10.1002/adma.202003598

delivered the cargo to ischemic brain tissue.^[14] This demonstrates that neutrophils can be used as carrier cells for drug delivery.^[15] Due to the involvement of inflammation and neutrophils in many diseases, loading neutrophils with drugs or drug-loaded nanocarriers *ex vivo* and reinjecting these hybrids into the patient has the potential of becoming a vital tool to deliver drugs locally to remote inflammatory sites despite systemic administration to dampen uncontrolled inflammation.

Here, we developed a neutrophil-mediated drug delivery system to deliver an anti-inflammatory agent encapsulated in a nanocarrier to the inflamed tissue. To this end, methotrexate (MTX), a potent immunosuppressive agent used to treat inflammatory and autoimmune diseases,^[16,17] was encapsulated in cationic liposomes (MTX-liposome) and loaded into isolated neutrophils *ex vivo* (MTX-liposome/neutrophils). We tested *in vitro* physiological functions of neutrophils after loading with MTX-liposomes. We characterized in detail the release of liposomes from loaded neutrophils and subsequent transport to target cells in an inflammatory environment. Fluorescence correlation spectroscopy (FCS) was employed to precisely measure the state of the released liposomes. Further, a combination of two-color flow cytometry and high-resolution fluorescence microscopy was used to show successful stimulated release and transport of loaded liposomes from neutrophils to target macrophages. The *in vivo* migratory behavior of loaded neutrophils was evaluated in a lipopolysaccharide (LPS)-injury skeletal muscle mouse model. Detailed analysis of the cell populations at the target site enabled detection of injected liposome-loaded neutrophils at the desired inflammatory site. The local anti-inflammatory effect intended through our hybrid system was demonstrated by measuring key cytokine levels at the target site. Moreover, a clinically relevant inflammatory mouse model of myocardial ischemia reperfusion injury (IRI) was employed to determine the versatility of loaded neutrophils migrating to the injured tissue. We envision that this system can serve as a universal platform to deliver a wide range of drugs including small chemical compounds (hydrophobic and hydrophilic), RNA, and proteins to inflamed tissue for improved regeneration.

Liposomes were chosen as an ideal nanocarrier candidate to encapsulate anti-inflammatory drugs due to high biocompatibility and the possibility to scale up the manufacturing process. MTX-loaded cationic liposomes were prepared using various drug concentrations with a diameter of ≈ 100 nm and a zeta potential of +30 mV to allow efficient cellular uptake (Figure 1a). Transmission electron microscopy (TEM) further confirmed that the size of MTX-liposomes was 111 ± 46 nm (Figure S1, Supporting Information). The loading yield was 1 wt% of MTX in liposomes. Retention of MTX inside liposomes was optimized to avoid premature exposure of neutrophils to the drug. At a cholesterol percentage of 40 wt%, only $\approx 5\%$ of the drug was released within the first 8 h, which was sufficiently stable for the intended application (Figure S2, Supporting Information, and Figure 1b). However, in a more complex biological environment, mimicked by incubating MTX-liposomes in 90% fetal bovine serum (v/v), $67 \pm 4\%$ of MTX was released from liposomes after 20 h incubation, reaching $85 \pm 7\%$ release after 52 h. This suggests timely release of MTX from liposomes after MTX-liposomes are released from neutrophils at the inflammatory site.

For the cellular component of the delivery system, we isolated neutrophils from mouse bone marrow and loaded them with liposomes *ex vivo* instead of targeting neutrophils with the nanocarrier *in vivo* to avoid off-target toxicity in healthy tissues and allow the administration of varying drug doses by injecting different numbers of neutrophils. Flow cytometry results (Figure 1c) confirmed a neutrophil purity of 95% and Giemsa–Wright staining (Romanowsky stain) revealed the typical lobular shape of the neutrophil nuclei (Figure 1d).

Different MTX concentrations inside the liposomes (5 mg mL^{-1} : MTX5; 10 mg mL^{-1} : MTX10, initial concentrations) and different lipid concentrations of liposomes (1 mg mL^{-1} : LP1; 2 mg mL^{-1} : LP2, initial concentrations) were incubated with neutrophils. Neutrophil viability was confirmed in all groups for 4 and 8 h incubation after loading (Figure S3, Supporting Information) and no morphological differences were shown by Giemsa–Wright staining (Figure 1d), which indicates high cytocompatibility of the chosen MTX-liposome formulation. Flow cytometry results showed more than 95% of neutrophils being positive for 1,1'-dioctadecyl-3,3,3',3'-tetramethylindodicarbocyanine (DiD)-labeled liposomes upon loading (Figure S4b, Supporting Information). Confocal laser scanning microscopy (CLSM) confirmed that most cells had taken up liposomes during the 1 h loading procedure (Figure 1e and Figure S4a, Supporting Information). 3D structural illumination microscopy (3D SIM) was employed to spatially localize MTX-liposomes within neutrophils, which revealed various locations of liposomes on or within the neutrophils (Figure 1f and Figure S4c, Supporting Information). In the context of medical applications, the most important characteristic is the final achieved drug loading per cell. The resulting loading capacity of MTX into neutrophils reached $0.2 \mu\text{g}$ per million cells (Figure 1g), which is the maximum loading capacity of MTX-liposomes onto neutrophils without affecting neutrophil viability and chemotaxis. This dose is sufficient for *in vivo* applications.^[18,19]

Next, we sought to test physiological functions of neutrophils after loading with MTX-liposomes. CD11b protein expression, superoxide generation, and cell migration behavior were assessed.^[8] CD11b is a neutrophil surface protein that mediates adhesion and migration function, which is upregulated once neutrophils are stimulated by inflammatory molecules in the blood.^[8] To mimic the environment encountered by neutrophils in the blood, we used a neutrophil chemotaxis peptide *N*-formyl-met-leu-phe (fMLP), which recruits neutrophils and subsequently initiates the inflammatory response at the site of tissue damage.^[20] As expected, CD11b expression levels of neutrophils and MTX-liposome/neutrophils significantly increased with increasing fMLP concentrations (Figure S5a, Supporting Information) and no significant differences were seen between blank neutrophils and liposome-loaded neutrophils. Superoxide is known to be released from neutrophils to kill microbes.^[21] Similarly, superoxide generation by neutrophils and liposome-loaded neutrophils was increased after treatment with fMLP and no significant differences were observed between blank neutrophils and liposome-loaded neutrophils (Figure S5b, Supporting Information). These results suggest that liposome-loading did not impair the ability of neutrophils to respond to inflammatory signals.

The migratory function of neutrophils was further tested *in vitro* using a transwell migration assay (Figure 2a), in which

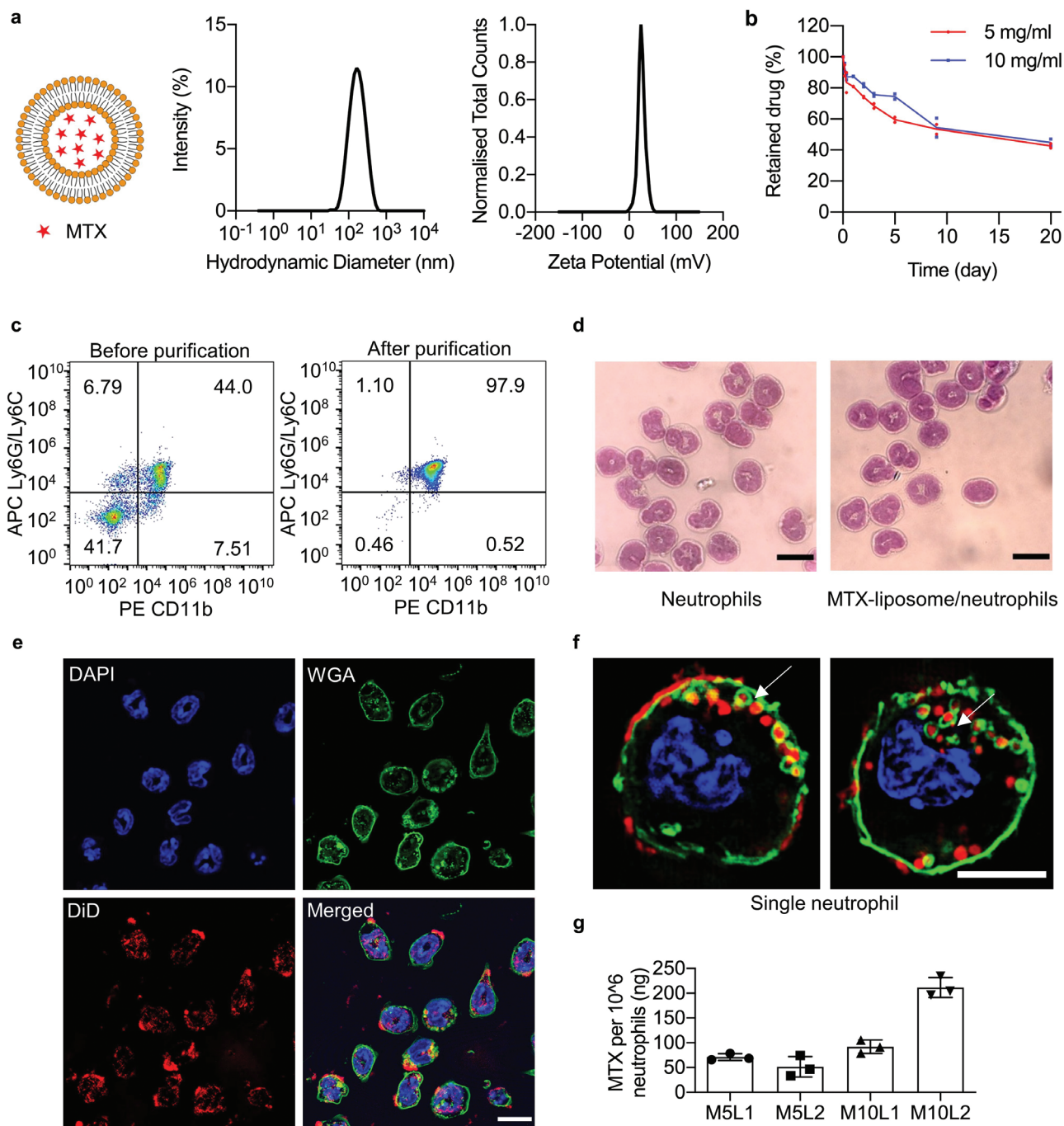


Figure 1. Preparation and characterization of MTX-liposome/neutrophils. a) Particle size measured by dynamic light scattering (DLS) and zeta potential distribution of MTX-liposomes. b) Quantity of retained drug inside liposomes over 20 days in PBS pH 7.4 at room temperature measured by LC–MS ($n = 2$ independent experiments). c) Flow cytometry analysis of the purity of isolated neutrophils before and after purification. Isolated neutrophils were double stained with PE anti-mouse CD11b and APC anti-mouse Ly6G/Ly6C antibodies. d) Morphological images of isolated neutrophils stained with Giemsa–Wright stain. Scale bar: 10 μm . e) CLSM images of MTX-liposome/neutrophils. The nuclei of neutrophils were stained with DAPI, the membranes of neutrophils were stained with WGA, and the liposomes were labeled with DiD. The merged image is the overlay of the three individual images. Scale bar: 10 μm . f) Super-resolution images (SIM) showing the location of MTX-liposomes on/in a single neutrophil. The arrows show various locations of liposomes on or within the neutrophil. Full image series in Figure S4c, Supporting Information. Scale bar: 5 μm . g) Quantity of MTX loaded in neutrophils after incubation with MTX-liposomes at different concentrations for 1 h as measured by ELISA (mean \pm SD, $n = 3$ independent experiments). M5: MTX 5 mg mL⁻¹; M10: MTX 10 mg mL⁻¹; L1: lipid concentration 1 mg mL⁻¹; L2: lipid concentration 2 mg mL⁻¹.

a porous membrane (pore size 3 μm) was used to study the migration ability of loaded neutrophils.^[22] After supplementation of fMLP to the basal medium, more cells migrated through

the pores of the transwell membrane (Figure 2b, Figure S6, Supporting Information). This indicates that after supplying fMLP, neutrophils were activated and migrated toward the

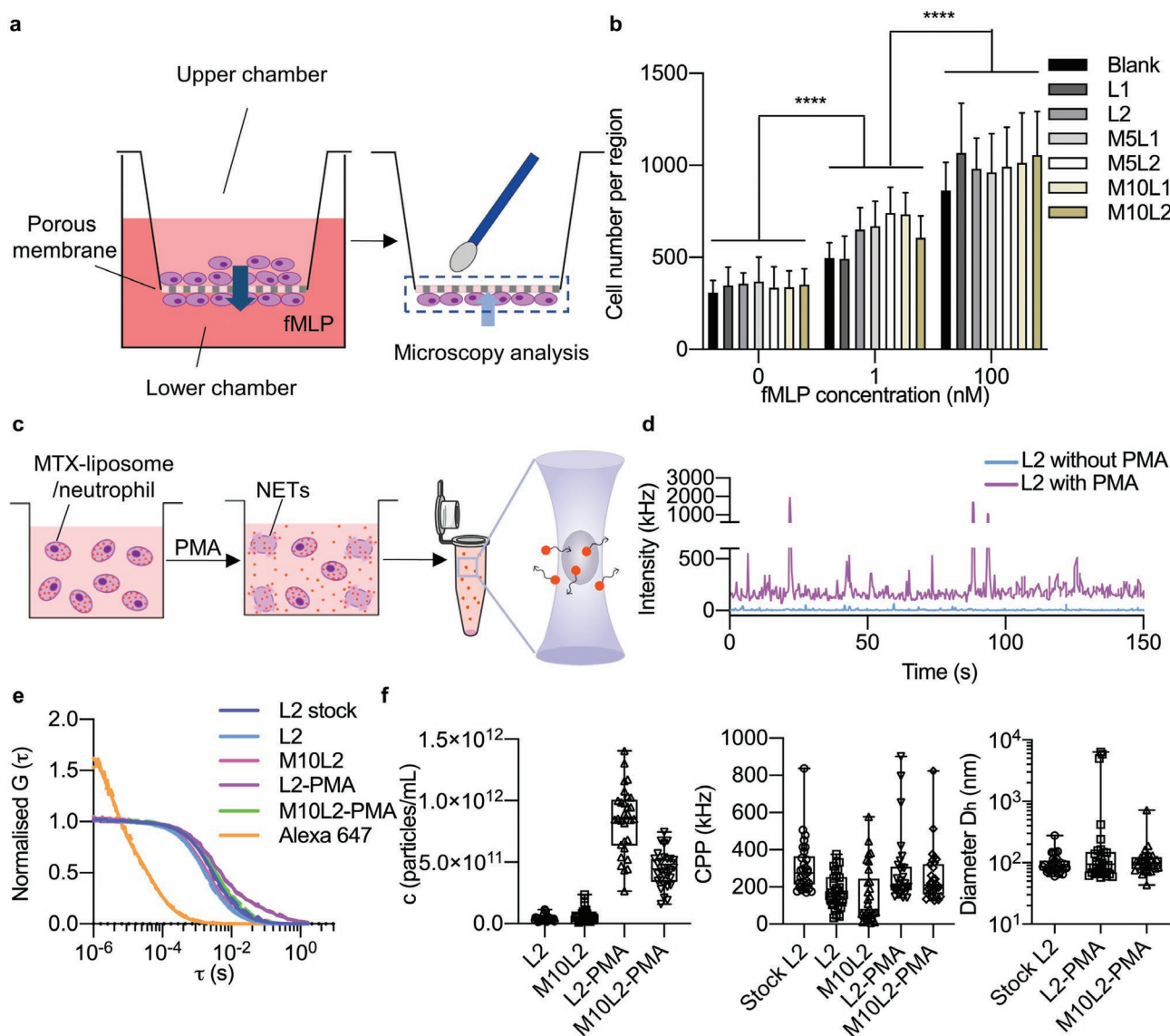


Figure 2. Migration ability of MTX-liposome-loaded neutrophils and stimulated release of liposomes (DiD-labeled) from neutrophils. a) Schematic illustration of the in vitro model to evaluate the migration capability of liposome/neutrophils across the porous membrane using a transwell assay. Neutrophils on the bottom side of the membrane were stained with DAPI and imaged using CLSM. b) Number of migrated neutrophils on the bottom side of the membrane (mean \pm SD, $n = 3$ independent experiments). **** $p < 0.0001$, two-way ANOVA, Bonferroni post hoc test. c) Schematic illustration of the FCS sample preparation. MTX-liposome/neutrophils were prepared and cultured with or without PMA for 8 h, followed by centrifugation to collect the supernatant. FCS measurements were performed to detect the amount and properties of liposomes after release from neutrophils. The graphic of the microcentrifuge tube was adapted from the Servier Medical Art website (Servier Medical Art by Servier is licensed under the CC-BY Creative Commons Attribution 3.0 Unported License (<https://creativecommons.org/licenses/by/3.0/>)). d) Raw fluorescence intensity traces recorded for samples collected after incubation of liposomes/neutrophils with and without stimulated release (+/-PMA). e) Average autocorrelation curves from FCS measurements ($n = 30$ independent measurements, 5 s each). f) Number of released liposomes given in particles per mL, signal (counts) per particle (CPP), and hydrodynamic diameter (D_h) of liposomes were calculated from the fit parameters obtained in (e). Center line, the median; box limits, upper and lower quartiles; whiskers, minimum and maximum values ($n = 30$ measurements per sample, repeat in Figure S5, Supporting Information).

higher fMLP concentration. Importantly, migrated neutrophils still contained DiD-labeled liposomes (Figure S7, Supporting Information), which shows that neutrophils carried their liposome cargo across the membrane. Taken together, these results show that after loading with MTX-liposomes, neutrophils maintained their physiological functions, which suggests that they can respond to inflammatory signals in the blood and migrate to the inflamed site, whilst carrying their cargoes.

We then explored the release of liposomes from neutrophils in the presence of fMLP (to mimic the chemotactic process) and phorbol myristate acetate (PMA) (to mimic the inflammatory site).^[13] After 8 h incubation, neutrophils formed NETs only in the PMA-containing medium as observed by CLSM (Figures S8 and S9, Supporting Information). An accompanying decrease in liposome signal inside neutrophils/NETs indicated that neutrophils underwent PMA-triggered NET

formation that caused the release of liposomes from neutrophils. Due to their small size, even liposomes loosely associated with neutrophil debris (NETs) will be prone to be uptaken by other cells, which yields the intended effect of delivering most of the liposomes to the target cells at the inflammatory site.

In order to quantify the amount and state of MTX-liposomes released from neutrophils into solution, we employed a sensitive, single-particle detection method called FCS, which allows to measure particles in complex environments, such as cell medium, containing proteins and cell debris (Figure 2c–f). After 8 h incubation, the detected raw fluorescence intensity was higher in supernatants of liposome-loaded neutrophils incubated in PMA-containing medium compared to samples from a non-inflammatory control environment (Figure 2d). The corresponding autocorrelation curves and calculated hydrodynamic diameters clearly show liposome release from the neutrophils (Figure 2e). The inflammatory environment induced by PMA caused an increase in liposome release as seen by the difference in particle counts compared to control (Figure 2f). Additional information on signal per liposome (counts per particle [CPP] in kHz) and diameter (D_h) of released liposomes revealed that there were no detectable differences between the original liposome solution and the released liposomes. Similar CPP values for the original liposomes and the PMA-released liposomes indicate that the same number of DiD molecules per liposome were retained during the loading/release processes. Only in some curves, partial aggregation of liposomes is found as indicated by high intensity bursts in the intensity trace (Figure 2d purple), a two-component autocorrelation curve (Figure 2e purple), and some outliers in the CPP and size plots (Figure 2f). This is expected due to the positively charged nature of the liposomes; it is not a concern for our type of delivery that protects the liposomes in neutrophils before reaching the target site. Furthermore, the amount of MTX in the released particle solution after incubation of loaded neutrophils in the presence of PMA was quantified by ELISA. 96% of loaded MTX was detected in the supernatant of MTX-liposomes-loaded neutrophils after incubation in the presence of PMA for 8 h (Figure S10, Supporting Information).

Next, we studied whether the released MTX-liposomes can subsequently be taken up by a target cell. This corresponds to the final destination of the nanocarrier where intracellular drug release should finally yield the desired therapeutic effect. Considering cell types present in the inflamed tissue, which can actively contribute to an uncontrolled immune response, a macrophage cell line (RAW 264.7 cells) was employed to represent target cells *in vitro*. MTX-liposome/neutrophils were co-cultured with macrophages for 8 h under physiological conditions (cell medium) or in the presence of an inflammatory environment (with PMA) (Figure 3a). We found that there was negligible rupture of neutrophils and release of MTX-liposomes at 8 h time point under non-inflammatory conditions (Figure S11, Supporting Information). However, in the presence of PMA an increased number of neutrophils died (stained by propidium iodide (PI)). Simultaneously, we observed the reuptake of MTX-liposomes by the target macrophages (Figure 3b). Nearly 82% of the macrophages contained MTX-liposomes (Figure 3c) as measured by flow cytometry. This indicates a successful transport cascade involving carrier neutrophils that undergo rupture to release and deliver the nanocarrier to target macrophages.

The final aspect involved in the delivery strategy is the drug effect on the target cells. Low concentrations of MTX inhibit folic acid synthesis, which slows down cell proliferation.^[23] Therefore, we assessed cell proliferation of the target cells (RAW 264.7) after co-culturing with MTX-liposome/neutrophils. RAW cells cultured with PMA and/or LPS grew 1.5-times faster compared to cells grown in basal medium (Figure 3d), while after applying MTX-liposome/neutrophils to macrophages in an inflammatory environment, the macrophage growth rate was reduced to a similar level seen when directly treated with free MTX using equivalent drug concentrations. The observed reduction in cell growth using our neutrophil-mediated delivery system confirms that sufficient amounts of drug were available for the desired immunosuppressive effect on target cells. Taken together, all *in vitro* data suggest an optimized delivery system amenable to loading a sufficient amount of MTX. Neutrophils remained viable and retained their physiological properties of adhesion and migration to allow for migration toward sources of inflammatory signals, inflammation-triggered release of drug-loaded liposomes, and subsequent liposome delivery to target cells.

Next, we investigated the *in vivo* migration ability of liposome-loaded neutrophils to remote inflammatory sites. In order to analyze the recruitment of *ex vivo* loaded neutrophils, we employed an inflammation model using LPS-induced tissue injury in mouse quadriceps, which has previously been demonstrated to cause upregulation in inflammatory gene expression.^[24] To induce skeletal muscle injury, we injected LPS intramuscularly to the right quadriceps of each mouse while the left untreated quadriceps served as healthy control. As previously reported, 24 h after LPS injection an acute inflammatory response was established in the LPS-injected muscle.^[24] At this time point, isolated neutrophils labeled with VivoTrack 680 were injected intravenously. Quadriceps from both legs were collected at the 1 h time point and processed to generate single cell suspensions that were analyzed using flow cytometry to identify neutrophils in the quadriceps (Figure 4a). Neutrophils accumulated in the LPS-injected quadriceps and accounted for 2.7% of total cells whereas only 0.03% of cells present in the healthy quadriceps were neutrophils (Figure 4b,d). This indicates that the intramuscular injection of LPS caused a local inflammatory response that resulted in neutrophil recruitment. We further analyzed the VivoTrack 680 signal based on the gated neutrophil population (only cells being positive for CD11b and Ly6G/Ly6C). Within the total neutrophil population in the LPS-injected quadriceps, 23% of neutrophils were positive for VivoTrack 680 (Figure 4b,d), which confirmed that injected neutrophils migrated to the inflamed tissue. In total, 0.53% of the total cell population collected from the LPS-injected quadriceps was injected neutrophils, which was expected as a large number of muscle and stroma cells are present in the quadriceps.

To study the time course of the neutrophil migration, we also collected quadriceps at 2 and 4 h after injection. In agreement with a previous study describing this model,^[24] we identified endogenous neutrophils at each time point in the LPS-injected quadriceps while there were only negligible number of neutrophils present in the healthy quadriceps (Figure 4d). Injected neutrophils were observed in the LPS-injected quadriceps 1 and 2 h after injection but no injected neutrophils were detected after 4 h (Figure 4d), which indicates that at the 4 h time point,

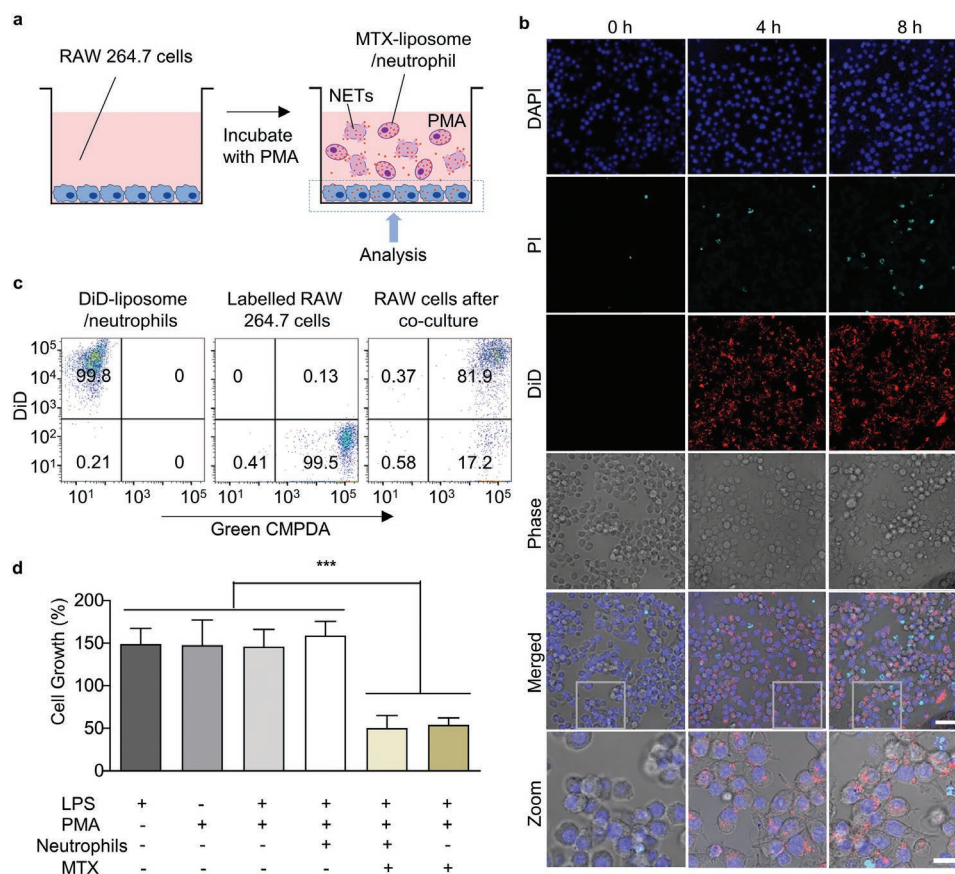


Figure 3. Neutrophil-mediated delivery and effect of MTX-liposome on co-cultured macrophages (RAW 264.7 cells). a) Schematic illustration of the in vitro co-culture system of macrophages (RAW 264.7 cells) and MTX-liposome/neutrophils. b) CLSM images of RAW 264.7 cells after incubation with liposome/neutrophils at 0, 4, and 8 h in presence of PMA (controls without PMA are in Figure S11, Supporting Information). The nuclei of RAW 264.7 cells were stained with DAPI, the released DNA fragments of neutrophils were stained with PI, and the liposomes were labeled with DiD. Scale bar: 50 μm . Zoom images, scale bar: 10 μm . c) Flow cytometry analysis of RAW 264.7 cells after co-culture with DiD-liposome/neutrophils. The green CMPDA channel shows RAW 264.7 cell labeling and the DiD channel represents liposome labeling. d) Proliferation of RAW 264.7 cells after treatment with inflammatory cytokines and co-culture with MTX-liposome/neutrophils compared to basal medium. Cell viability was measured using Cell Counting Kit-8 (mean \pm SD, $n = 3$ independent experiments). *** $p < 0.001$, one-way ANOVA, Bonferroni post hoc test.

the injected neutrophils in the quadriceps may have formed NETs or may have only transiently adhered to the capillaries in the tissue. Thus, most of the injected labeled neutrophils were recruited to the inflamed quadriceps within 2 h after injection. Neutrophil recruitment from bone marrow, liver, and spleen and transmigration into tissue usually takes 2–16 h.^[25] However, when injecting isolated neutrophils directly into the bloodstream at the peak of inflammation, this process may happen faster. We also analyzed blood samples collected at each time point by flow cytometry. The results mirrored the results from muscle samples. We detected injected neutrophils at the 1 and 2 h time points (Figure 4d). This indicates that the injected neutrophils were circulating in the blood up to 2 h after injection.

Subsequently, we loaded isolated VivoTrack 680-labeled neutrophils with DiL-labeled liposomes as described above to test if these neutrophils can also carry particles to the inflamed muscles. After analyzing the VivoTrack 680 and DiL signals based on the gated neutrophil population, we found that 98% of the injected neutrophil population contained DiL-labeled liposomes in the LPS-injected quadriceps (Figure 4c and Figure S12b, Supporting Information), whilst none were found in the healthy

quadriceps. This suggests that liposome-loaded neutrophils retain their ability to migrate to inflamed tissue in vivo and carry liposomes for potential delivery to target cells. Furthermore, the total population of DiL positive cells among total cells digested from the LPS-injected quadriceps was larger than that of DiL positive CD11b+Ly6G/Ly6C+VivoTrack 680+ neutrophils only (Figure S13, Supporting Information). No DiL positive cells were detected in the healthy quadriceps. This suggests that the cargo DiL was delivered to other cells in the inflamed quadriceps.

Since we observed that liposome-loaded neutrophils can migrate and deliver their cargo to inflamed tissue, we explored the anti-inflammatory effect of our hybrid system MTX-liposome/neutrophils. We measured the inflammatory cytokines IL-6, IL-1 α , and TNF- α 48 h after LPS injection, because MTX used to treat inflammatory diseases alters their expression levels.^[26,27] As expected, IL-6 and TNF- α levels increased in the LPS-injected quadriceps compared to the control muscle, while IL-1 α remained at baseline levels (Figure 4e and Figure S14, Supporting Information). Thus, we subsequently used IL-6 and TNF- α as indicators of inflammation. 10 million neutrophils loaded with MTX-liposomes were then injected into LPS-treated

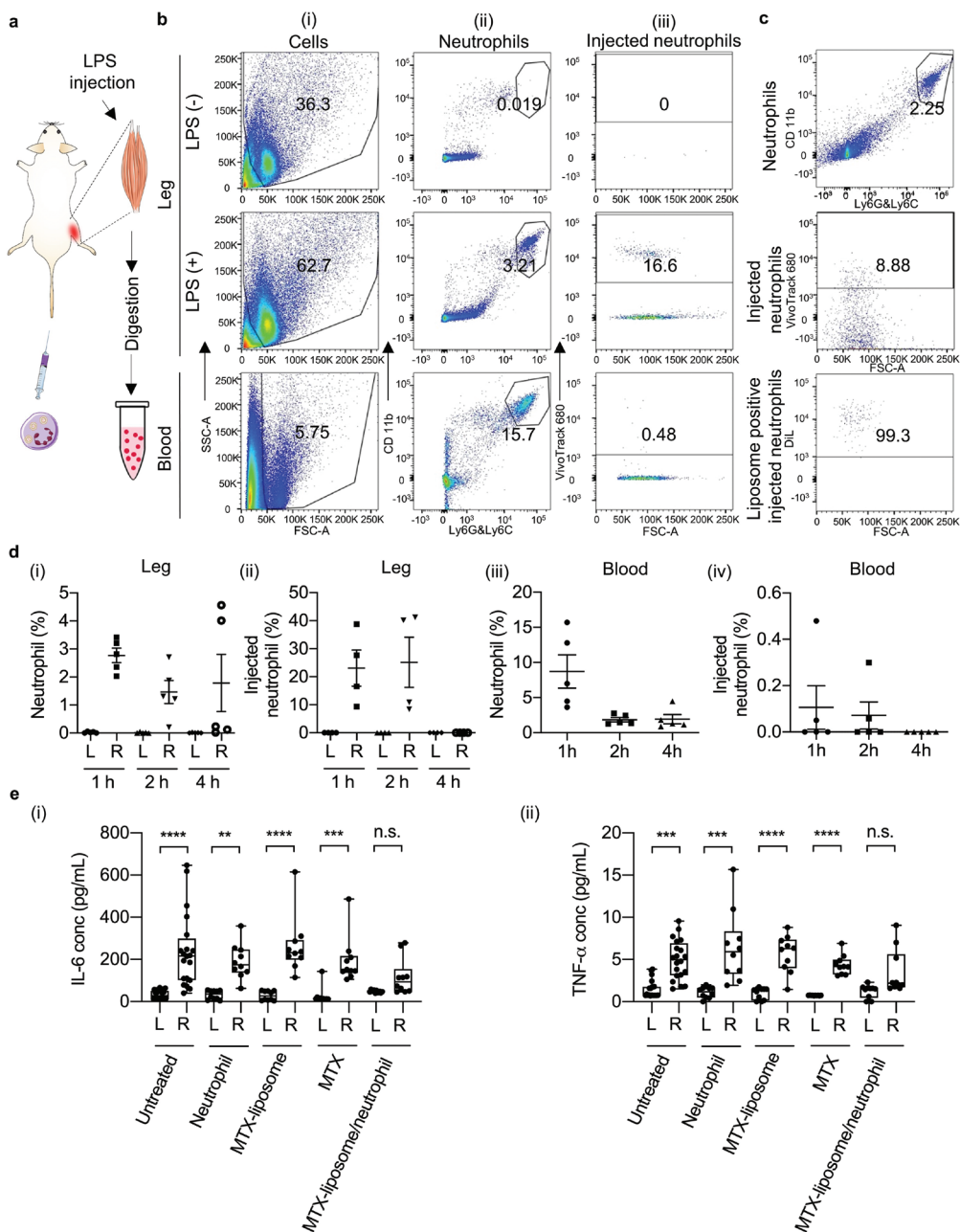


Figure 4. Targeting effect of MTX-liposome/neutrophils on the LPS-injected muscle and the resulting mitigation of inflammation. a) Schematic illustration showing the sample preparation process of quadriceps from LPS-treated mice after i.v. injection of liposome/neutrophils (liposomes were labeled with DiI and neutrophils were labeled with VivoTrack 680) for flow cytometry analysis. The graphics of syringe and muscle were adapted from the Servier Medical Art website (Servier Medical Art by Servier is licensed under the CC-BY Creative Commons Attribution 3.0 Unported License (<https://creativecommons.org/licenses/by/3.0/>)). b) Flow cytometry analysis of digested quadriceps after neutrophil injection (labeled with VivoTrack 680). An example of gating strategy was shown in Figure S12a, Supporting Information. (i) Forward scatter versus side scatter plots for total counted events; gate excludes cell doublets and red blood cells. (ii) PE anti-mouse CD11b and Alexa 488 anti-mouse Ly6G/Ly6C plots for neutrophils. Gate shows the double positive population of neutrophils. For quadriceps samples, the gating area was chosen based on the quadriceps sample from untreated mouse; for blood samples, the gating area was chosen based on the blood sample from untreated mouse. (iii) Forward scatter versus VivoTrack 680 plots for injected neutrophils (CD11b+Ly6G/Ly6C+). Gate shows the VivoTrack 680 positive population of injected neutrophils compared to the total neutrophil population. c) Flow cytometry analysis of quadriceps after injection of liposome-loaded neutrophils (liposomes were labeled with DiI and neutrophils were labeled with VivoTrack 680). DiI analysis was based on the gated CD11b+Ly6G/Ly6C+VivoTrack 680+ neutrophil population. d) (i) Neutrophil percentage of total cell population in the healthy quadriceps (L) and LPS-injected quadriceps (R) at 1, 2, and 4 h post neutrophil injection. (ii) Percentage of injected neutrophils within total neutrophil population in the healthy quadriceps (L) and LPS-injected quadriceps (R) at 1, 2, and 4 h post neutrophil injection. Data shown as mean \pm SEM, $n = 5$. e) (i) IL-6 levels and (ii) TNF- α levels in the healthy quadriceps and LPS-injected quadriceps after different treatments. Center line, the median; box limits, upper and lower quartiles; whiskers, minimum and maximum values. ** $p < 0.01$, *** $p < 0.001$, **** $p < 0.0001$, n.s. = not significant, Kruskal–Wallis, Corrected Dunn’s post hoc test, $n = 20$ in the untreated group, $n = 10$ in other treated groups.

mice, which correspond to an amount of 2 µg of MTX per mouse. This dose was previously found to be sufficient to mitigate inflammation.^[28,29] After 24 h, quadriceps from both legs were collected and cytokine levels were measured by Luminex assay. MTX-liposome/neutrophils treatment reduced IL-6 levels in the LPS-injected quadriceps to levels comparable to those in the healthy quadriceps in most animals, while levels in control groups stayed elevated (Figure 4e[i]). An equivalent amount of MTX injection did not downregulate cytokine levels in the LPS-injected quadriceps (Figure 4e[i]). MTX-liposomes by themselves did not have a beneficial effect, and those mice still had significantly higher cytokine levels in the LPS-injected quadriceps. This is likely due to the positive charge on the liposome surface which resulted in rapid clearance of the MTX-liposomes from the bloodstream after injection.^[30] If MTX-liposomes are loaded into neutrophils, they are protected and carried to the inflamed muscle and are then locally released to mitigate inflammation. These results further confirmed that injected neutrophils locally delivered loaded MTX-liposomes to the inflamed quadriceps resulting in the desired anti-inflammation effects, while free MTX and MTX-liposomes did not have any beneficial effect because they were not able to efficiently reach the tissue without the carrier neutrophils. Comparing the fold change of IL-6 in the LPS-injected versus non-injected quadriceps between the control and various treatment groups, we observed that only MTX-liposome/neutrophil treatment had significantly lowered the levels of IL-6 in the inflamed quadriceps compared to the untreated control group (Figure S15, Supporting Information), suggesting the benefit of the neutrophil-based drug delivery. TNF-α levels were also significantly increased in the LPS-injected leg of all the control groups (Figure 4e[ii]), but not in the MTX-liposome/neutrophil group, which further confirms that only the MTX-liposome/neutrophil treatment resulted in beneficial effects. However, TNF-α levels did not increase as much as IL-6 levels after LPS injection, indicating that IL-6 is the superior experimental readout in this model.

Taken together, in vivo migration and treatment studies of our neutrophil-mediated MTX-liposome delivery system demonstrated that loaded neutrophils can migrate to inflamed target

tissue in vivo. Upon arrival in the inflamed tissue, neutrophils release the drug-loaded liposomes causing the intended anti-inflammatory effect.

Furthermore, we applied this system to a clinically relevant inflammation model of myocardial IRI to determine the versatility of neutrophil-mediated delivery to the site of inflammation. After VivoTrack 680-labeled neutrophils were i.v. injected into mice with myocardial IRI and healthy control mice (Figures S16 and S17, Supporting Information), a significantly higher amount of VivoTrack 680 dye from injected neutrophils was detected in IRI hearts compared to healthy hearts for both 1 and 2 h time points (hearts were perfused with PBS to remove non-infiltrated neutrophils). Some VivoTrack 680 signal was also detected in all other tested organs in mice with myocardial IRI, mainly in the liver and spleen. This might be due to systemic inflammation after acute MI, which induced the migration of neutrophils to other organs,^[31] or caused premature NET formation in the blood with neutrophil debris ending up in the mononuclear phagocyte system of the liver and spleen.

More importantly, the ability of neutrophils to carry liposomes to the injured hearts was investigated. We injected liposomes (labeled with DiD)-loaded neutrophils and collected organs 1 h post injection. The IRI hearts showed significantly higher DiD fluorescence signal from liposomes than the other two groups (Figure 5), which reveals accumulation of liposomes in the injured hearts by using the neutrophil-mediated strategy. The DiD signal also appeared in other organs (Figure S18, Supporting Information), which can be explained as above (Figures S16 and S17, Supporting Information) by systemic inflammation and premature NET formation. These findings suggest versatility of the neutrophil-mediated delivery strategy that is promising to be applied in the myocardial IRI model, an inflammatory disease model with longer disease progression period and higher relevance to human disease.

In this report, we have presented a neutrophil-mediated drug delivery system taking advantage of the physiological properties of neutrophils to carry anti-inflammatory drug-loaded liposomes to remote inflammatory sites. We have shown that after loading sufficient amount of MTX-liposomes, the treated

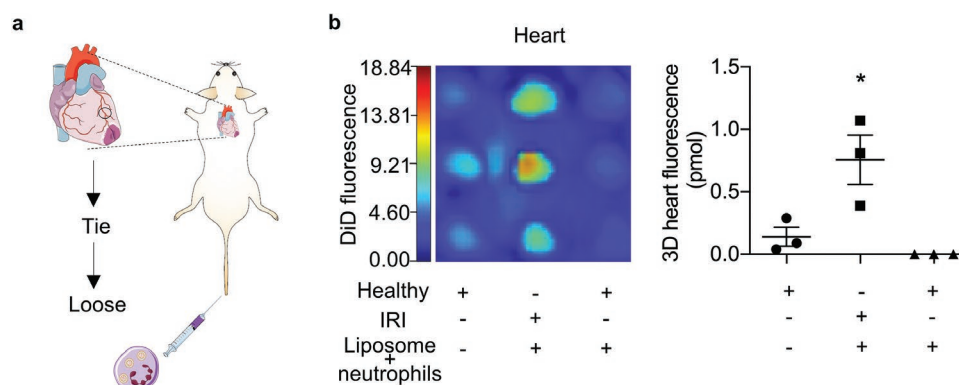


Figure 5. Neutrophil-mediated liposome delivery to the IRI heart. a) Schematic illustration showing the myocardial IRI surgery and i.v. injection of liposome/neutrophils (liposomes were labeled with DiD). The graphics of hearts were adapted from the Servier Medical Art website (Servier Medical Art by Servier is licensed under the CC-BY Creative Commons Attribution 3.0 Unported License (<https://creativecommons.org/licenses/by/3.0/>)). b) In vivo accumulation of liposomes in the heart after myocardial IRI surgery at 1 h post liposome/neutrophil injection. Left: DiD signal in hearts from mice at 1 h post liposome/neutrophil injection (liposomes were labeled with DiD); Right: Total amount of DiD dye in hearts (pmol, mean ± SEM). * $p < 0.05$, one-way ANOVA, Bonferroni post hoc test, $n = 3$.

neutrophils maintained their adhesion and migration functions in response to inflammatory signals after loading with MTX-liposomes. Detailed in vitro tests revealed the release of liposomes from neutrophils and their subsequent uptake by target macrophages in an inflammatory environment. This system was further demonstrated in vivo showing neutrophils can carry loaded liposomes and migrate to the inflammatory site presumably by responding to chemoattractant signals in the blood and accumulate in the inflamed tissue. Furthermore, we loaded MTX in this system and deployed MTX-liposome/neutrophils in vivo in the same LPS-injury skeletal muscle model and successfully decreased levels of IL-6 and TNF- α in the inflamed muscle. Finally, the versatility of neutrophil-mediated liposome delivery to the inflamed tissue was demonstrated in the myocardial IRI model showing successful liposome delivery to the injured hearts via neutrophils.

The effects of our MTX-liposome/neutrophil system on inflammatory cytokine levels suggest increased delivery of MTX compared to the controls. We would like to highlight two possible mechanisms for improved delivery. (i) Neutrophils might have transmigrated across the endothelial barrier together with the cargo, where it was released. (ii) Neutrophils could have adhered to the blood vessels of the inflamed tissue and released cargo locally, which might have entered the inflamed tissue on its own or via other cells. These two proposed mechanisms warrant future studies on the behavior of injected neutrophils after they arrive at the inflammatory site. This will provide additional mechanistic insight into the neutrophil-mediated drug delivery strategy to inflamed tissue. Furthermore, increasing the MTX injection dose could improve the treatment efficacy, which can be achieved by either injecting a higher dose or several doses of MTX-liposome/neutrophils or choosing another nanocarrier with longer drug retention times to increase the MTX loading capacity. If injecting more neutrophils, the effect of neutrophils themselves needs to be evaluated carefully as excessive neutrophils might cause excess inflammation.

A major advantage of our system is that we used simple liposomes combined with neutrophils to achieve local drug delivery using a one-step incubation method, which offers additional benefits including improved reproducibility and robustness. This neutrophil-based delivery system offers the versatility to use different types of nanoparticles, for example, stimuli-responsive micelles or polymersomes that can allow encapsulation of various drug doses, other drugs, and additionally incorporate triggered release in the target cells. Different drugs loaded inside nanoparticles give possibilities of loading therapeutic combinations to reduce tissue inflammation and actively promote repair at the same time. Moreover, this system encourages the future prospect of using different immune cells involved in inflammation such as macrophages and T cells as carrier cells to deliver therapeutics at different stages of inflammation, opening new opportunities for different therapeutic treatments in inflammatory diseases.

Supporting Information

Supporting Information is available from the Wiley Online Library or from the author.

Acknowledgements

J.C. acknowledges support from the China Scholarship Council. A.N. acknowledges support from his previous Swiss National Science Foundation Early Postdoc Mobility Fellowship (P2BSP2_168751) and current Sir Henry Wellcome Postdoctoral Fellowship (209121_Z17_Z) from the Wellcome Trust. A.K.B. acknowledges support from her Marie Skłodowska-Curie Individual Fellowship funded by the European Commission H2020 (No. 794059). C.W.W. acknowledges support from the Biotechnology and Biological Sciences Research Council Doctoral Training Partnership (BB/N503952/1). T.J.K. acknowledges the European Union's Horizon 2020 research and innovation programme under the Marie Skłodowska-Curie Individual European Fellowship (Grant Agreement No. 746980). S.S. acknowledges the BHF project grant (PG/16/93/32345). M.M.S. acknowledges support from the grant from the UK Regenerative Medicine Platform "Acellular/Smart Materials – 3D Architecture" (MR/R015651/1). M.D.S. acknowledges support from British Heart Foundation (CH/08/002/29257). This project has received funding from the European Union's Horizon 2020 for Research & Innovation program under grant agreement No. 681137 for R.J.S. and P.F.M. The sole responsibility for the content of this project lies with the authors. It does not necessarily reflect the opinion of the European Union. The European Commission is not responsible for any use that may be made of the information contained therein. The authors acknowledge the support from The Facility for Imaging by Light Microscopy (FILM) and Department of Materials Harvey Flower Microscopy Suite at Imperial College London. The Light Microscopy Facilities at the Francis Crick Institute London are acknowledged for providing access to FCS. The authors thank Dr. Ilaria Malanchi for the critical reading of and commenting on the manuscript. The authors acknowledge support from the Imperial BHF Centre for Cardiac Regenerative Medicine (RM/17/1/33377). Raw data is available upon reasonable request from rdm-enquiries@imperial.ac.uk.

Conflict of Interest

The authors declare no conflict of interest.

Author Contributions

J.C., T.J.K., S.S., and M.M.S. conceived the idea and designed the experiments. J.C. performed the majority of experimental work. A.N. performed the FCS measurement and analysis. A.K.B., P.F.M., and R.J.S. assisted with the design of the in vivo experiments and performed the LPS-injury skeletal muscle model. M.B. and M.D.S. performed the myocardial IRI model. C.W.W. performed the SIM imaging. A.S. and S.S. assisted with neutrophil isolation and FMT tracking experiments. J.T. performed the TEM imaging. J.C., A.N., and S.S. wrote the manuscript with feedback from all the authors. S.S., A.N., T.J.K., and M.M.S. supervised the project.

Keywords

inflammation, liposomes, methotrexate, neutrophils

Received: May 26, 2020
Revised: September 3, 2020
Published online: October 26, 2020

-
- [1] L. Chen, H. Deng, H. Cui, J. Fang, Z. Zuo, J. Deng, Y. Li, X. Wang, L. Zhao, *Oncotarget* **2018**, 9, 7204.
[2] I. Manabe, *Circ. J.* **2011**, 75, 2739.

- [3] W. Badri, K. Miladi, Q. A. Nazari, H. Greige-Gerges, H. Fessi, A. Elaissari, *Int. J. Pharm.* **2016**, 515, 757.
- [4] H. E. Vonkeman, M. A. F. J. van de Laar, *Semin. Arthritis Rheum.* **2010**, 39, 294.
- [5] W. M. Pardridge, *J. Cereb. Blood Flow Metab.* **2012**, 32, 1959.
- [6] E. Blanco, H. Shen, M. Ferrari, *Nat. Biotechnol.* **2015**, 33, 941.
- [7] S. Tenzer, D. Docter, J. Kuharev, A. Musyanovych, V. Fetz, R. Hecht, F. Schlenk, D. Fischer, K. Kiouptsi, C. Reinhardt, K. Landfester, H. Schild, M. Maskos, S. K. Knauer, R. H. Stauber, *Nat. Nanotechnol.* **2013**, 8, 772.
- [8] J. Xue, Z. Zhao, L. Zhang, L. Xue, S. Shen, Y. Wen, Z. Wei, L. Wang, L. Kong, H. Sun, Q. Ping, R. Mo, C. Zhang, *Nat. Nanotechnol.* **2017**, 12, 692.
- [9] C. Cole, J. Qiao, T. Kottke, R. M. Diaz, A. Ahmed, L. Sanchez-Perez, G. Brunn, J. Thompson, J. Chester, R. G. Vile, *Nat. Med.* **2005**, 11, 1073.
- [10] J. E. Park, J. Jang, J. H. Choi, M. S. Kang, Y. J. Woo, Y. R. Seong, C. B. Choi, H. S. Lee, S. C. Bae, Y. S. Bae, *J. Immunol. Res.* **2015**, 2015, 834085.
- [11] M. Phillipson, P. Kubes, *Nat. Med.* **2011**, 17, 1381.
- [12] A. Mantovani, M. A. Cassatella, C. Costantini, S. Jaillon, *Nat. Rev. Immunol.* **2011**, 11, 519.
- [13] V. Brinkmann, U. Reichard, C. Goosmann, B. Fauler, Y. Uhlemann, D. S. Weiss, Y. Weinrauch, A. Zychlinsky, *Science* **2004**, 303, 1532.
- [14] J. Hou, X. Yang, S. Li, Z. Cheng, Y. Wang, J. Zhao, C. Zhang, Y. Li, M. Luo, H. Ren, J. Liang, J. Wang, J. Wang, J. Qin, *Sci. Adv.* **2019**, 5, eaau8301.
- [15] D. Chu, X. Dong, X. Shi, C. Zhang, Z. Wang, *Adv. Mater.* **2018**, 30, 1706245.
- [16] A. K. Agarwal, M. Wali, S. Chandra, A. Jain, S. Wadhwa, *J. Assoc. Physicians India* **1994**, 42, 888.
- [17] E. E. Lower, R. P. Baughman, *Arch. Intern. Med.* **1995**, 155, 846.
- [18] B. N. Cronstein, D. Naime, E. Ostad, *J. Clin. Invest.* **1993**, 92, 2675.
- [19] H. To, H. Yoshimatsu, M. Tomonari, H. Ida, T. Tsurumoto, Y. Tsuji, E. Sonemoto, N. Shimasaki, S. Koyanagi, H. Sasaki, I. Ieiri, S. Higuchi, A. Kawakami, Y. Ueki, K. Eguchi, *Chronobiol. Int.* **2011**, 28, 267.
- [20] D. Feng, J. A. Nagy, K. Pyne, H. F. Dvorak, A. M. Dvorak, *J. Exp. Med.* **1998**, 187, 903.
- [21] C. C. Winterbourn, A. J. Kettle, M. B. Hampton, *Annu. Rev. Biochem.* **2016**, 85, 765.
- [22] J. M. Paulsson, S. H. Jacobson, J. Lundahl, *J. Immunol. Methods* **2010**, 361, 82.
- [23] E. S. L. Chan, B. N. Cronstein, *Arthritis Res. Ther.* **2002**, 4, 266.
- [24] P. F. McKay, D. Cizmeci, Y. Aldon, J. Maertzdorf, J. Weiner, S. H. E. Kaufmann, D. J. M. Lewis, R. A. van den Berg, G. D. Giudice, R. J. Shattock, *eLife* **2019**, 8, e46149.
- [25] E. Kolaczowska, P. Kubes, *Nat. Rev. Immunol.* **2013**, 13, 159.
- [26] B. N. Cronstein, *Rheum. Dis. Clin. North Am.* **1997**, 23, 739.
- [27] H. Tian, B. N. Cronstein, *Bull. NYU Hosp. Jt. Dis.* **2007**, 65, 168.
- [28] H. To, S. Irie, M. Tomonari, Y. Watanabe, T. Kitahara, H. Sasaki, *J. Pharm. Pharmacol.* **2009**, 61, 1333.
- [29] J. D. Heilborn, M. Stahle-Backdahl, F. Albertioni, I. Vassilaki, C. Peterson, E. Stephansson, *J. Am. Acad. Dermatol.* **1999**, 40, 741.
- [30] T. Ishida, H. Harashima, H. Kiwada, *Biosci. Rep.* **2002**, 22, 197.
- [31] L. Fang, X. L. Moore, A. M. Dart, L. M. Wang, *J. Geriatr. Cardiol.* **2015**, 12, 305.